

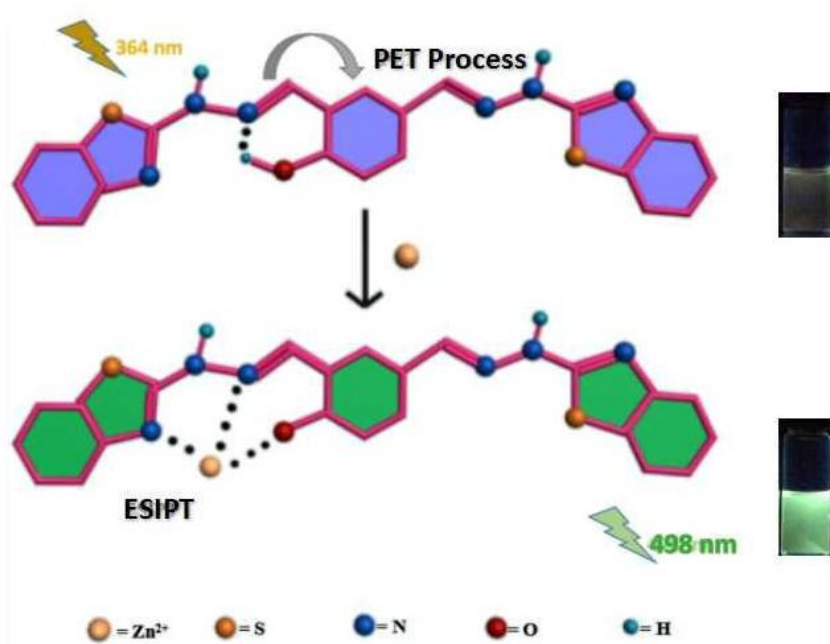
A new fluorescence chemosensor based on benzothiazole derivative for Zn²⁺ and its logic gate behavior

Jing-Han Hu*, Jing Qi, You Sun, Peng-Xiang Pei

College of Chemical and Biological Engineering, Lanzhou Jiaotong University, Lanzhou, Gansu, 730070, P. R. China

E-mail: hujinghan62@163.com

Abstract: A novel benzothiazole derivative **J** as a fluorescent chemosensor for Zn²⁺ has been designed and synthesized. The chemosensor **J** exhibits high selectivity and sensitivity to Zn²⁺ as fluorescence “turn-on” behavior, which the other cations do not make sense. The detection limit calculated by fluorescence titration method was 1.64×10^{-8} M. Furthermore, the generated **J**-Zn²⁺ ensemble could recover the enhanced fluorescence upon the addition of EDTA generating an “on-off-on” recycle. In addition, the test strip based on **J** was fabricated, which could act as a convenient and efficient Zn²⁺ test kit.



Keywords: Benzothiazole; Chemosensor; Zinc (Zn²⁺); Logic gate behavior;

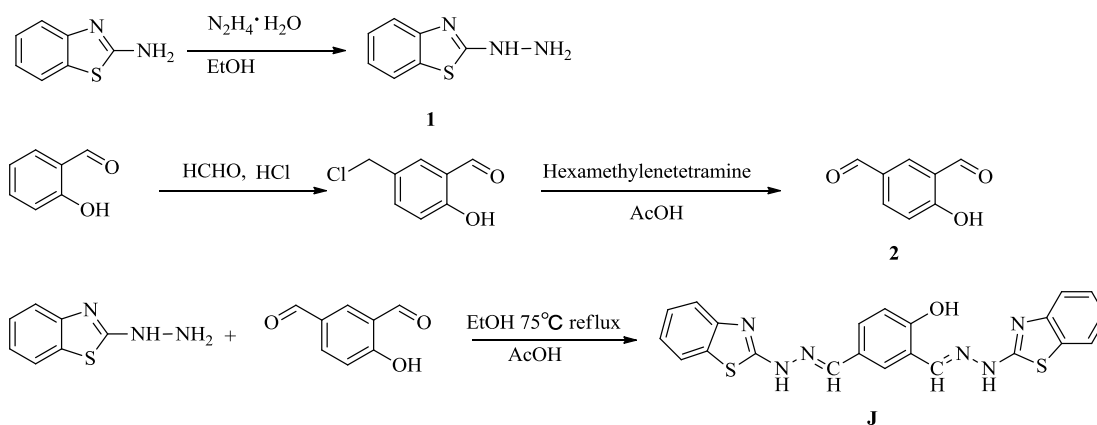
Introduction

Recently, the design and exploration of fluorescent sensors for detecting transition metal ions have received more attention due to their advantages of high selectivity, sensitivity, and real-time monitoring other methods.¹⁻³ Zinc as the second most abundant and essential transition metal in the human body influences many important physiological functions in biological activities such as gene expression, neural signal transmission, DNA binding or recognition, cell apoptosis and immune function.⁴⁻⁹ Lack or excess of zinc level in the human body may cause physiological or pathological changes and produce varieties of diseases. The total concentration of zinc ion in serum should be 10 μM .¹⁰⁻¹² At present, a range of detection methods for zinc ion have been developed such as inductive and coupled plasma mass spectrometry, atomic absorption spectrometry, which may be time-consuming or need use some sophisticated instrumentation.¹³⁻¹⁶ Accordingly, developing simple, selective and sensitive detection tools for Zn^{2+} in living organisms is challenging.

Until now, a number of fluorescent sensors for Zn^{2+} based on various fluorophores such as coumarin, quinoline, naphthalene, pyrene, and nanoparticles have been reported.¹⁷⁻²² Nevertheless, only a few related literatures about sensors for the zinc ion based on the thiazole group could be found.²³⁻²⁶ Benzothiazole derivatives could provide an electron-rich environment and good ligating ability.²⁷⁻²⁸

In view of the investigations and as a part of our research interests in molecular recognition,²⁹⁻³² we have designed and synthesized a new benzothiazole derivative **J** (2, 4-bis-[[[(2-benzothiazolythio)-hydrazinylidene] methyl] phenol) as a selective fluorescent sensor for Zn^{2+} . It could achieve the recognition purpose by inhibition of photoinduced electron transfer

(PET) and excited-state intramolecular proton transfer (ESIPT) effect. **J** showed a large fluorescence enhancement at 498 nm in the presence of Zn^{2+} in DMSO/ H_2O (pH=7.2, v/v=4:1) HEPES buffer solutions. The detection process of Zn^{2+} usually was interfered by Mg^{2+} , especially Cd^{2+} . Fortunately, the sensor **J** could detect and distinguish Zn^{2+} without their interference. Lin et al.³³ reported a similar sensor for Zn^{2+} . Therefore we have compared the two compounds listed in Table S 1 (Supplemental Materials). The results showed that **J** could detect Zn^{2+} in higher water-content system. And **J** had a fluorescence response between pH 5 and 11. The mechanism of the detection process was verified by spectroscopic methods including ^1H NMR, UV-vis, and mass spectrometry.



Scheme 1 Synthesis of the sensor molecule **J**.

Results and discussion

In order to investigate the Zn^{2+} recognition abilities of the sensor **J**, we carried out a series of host-guest recognition experiments in DMSO/ H_2O (pH = 7.2, v/v = 4:1) HEPES buffer solutions. The chemosensor **J** was tested with aqueous solutions of the perchlorate salts of all common cationic analytes such as Fe^{3+} , Hg^{2+} , Ag^+ , Ca^{2+} , Cu^{2+} , Co^{2+} , Ni^{2+} , Cd^{2+} , Pb^{2+} , Zn^{2+} , Cr^{3+} , and Mg^{2+} . As shown in Figure 1, in the fluorescence spectrum, the emission of **J** appeared at the

maximum emission wavelength was 498 nm when excited at $\lambda_{\text{ex}} = 364$ nm. Upon the addition of Zn^{2+} ions (20 equiv.), the fluorescence intensity of sensor **J** increased, in which the color change from colorless to bright green could be distinguished by the naked eye under a UV-vis lamp. None of other ions (Fe^{3+} , Hg^{2+} , Ag^+ , Ca^{2+} , Cu^{2+} , Co^{2+} , Ni^{2+} , Cd^{2+} , Pb^{2+} , Cr^{3+} , and Mg^{2+}) induced any significant changes in the fluorescence spectrum of the sensor **J**.

Further, to evaluate the selectivity of **J**, we measured the fluorescence intensity of **J** in the presence of other cations such as Fe^{3+} , Hg^{2+} , Ag^+ , Ca^{2+} , Cu^{2+} , Co^{2+} , Ni^{2+} , Cd^{2+} , Pb^{2+} , Cr^{3+} and Mg^{2+} (4×10^{-4} M) including Zn^{2+} ion. (Figure 2) Therefore, it was clear that interference of other ions was negligibly small during the detection of Zn^{2+} .

Figure 1 (a) Fluorescence emission data for **J** and in the presence of various metal ions in DMSO/ H_2O (pH = 7.2, v/v = 4:1) HEPES buffer solutions. ($\lambda_{\text{ex}} = 364$ nm). (b) Color changes observed upon the addition of various cations (20 equiv.) to solutions of sensor **J** (2×10^{-5} M) in DMSO/ H_2O (pH = 7.2, v/v = 4:1) HEPES buffer solutions.

Figure 2 Fluorescence intensity changes of the **J** ($20 \mu\text{M}$) to Zn^{2+} (20 equiv.) in the presence of various test cations (20 equiv.) in DMSO/ H_2O (pH = 7.2, v/v = 4:1) HEPES buffer solutions.

The interaction between probe **J** and Zn^{2+} was also investigated in the fluorescence emission spectra in DMSO/ H_2O (pH = 7.2, v/v=4:1) HEPES buffer solutions. It was recorded during the titrations with different concentrations of Zn^{2+} 0 – 2 equivalent. As shown in Figure 3, when **J** was treated with 1.6 equivalent of Zn^{2+} , the fluorescence intensity at 498 nm would keep stable and almost change no more.

The detection limit is one of the most important parameters in ion sensing. The fluorimetric detection limits of sensor **J** for Zn^{2+} were also determined. As shown in Figure S 4, the minimum concentration of Zn^{2+} for fluorescence detection by the naked – eye was 1.00×10^{-7} M, by using a UV – vis lamp at 365 nm. In the meantime, the detection limit of the fluorescence spectra measurements was 1.64×10^{-8} M for Zn^{2+} , (Figure S 5) as calculated on the basis of $3S_B/S$ (where S_B is the standard deviation of the blank solution and S is the slope of the calibration curve). Thus, **J** can be applied to detect Zn^{2+} at an extremely low concentration level of 10^{-7} M, which may fully satisfy the requirements in biosensing, as labile Zn^{2+} in the human body was reported to exist at a millimolar concentration level.³⁴⁻³⁵ These data indicated that probe **J** showed high sensitivity toward Zn^{2+} . Moreover, the association constant for Zn^{2+} was found to be 6.62×10^4 M^{-1} in the same media.³⁶

Figure 3 Fluorescence spectra of **J** (20 μM) in the presence of different concentration of Zn^{2+} (0 – 2 equiv.) in DMSO/ H_2O (pH = 7.2, v/v = 4:1) HEPES buffer solutions. Inset shows a plot of fluorescence intensity depending on the concentration of Zn^{2+} in the range from 0 to 2 equivalents.

Generally, the reactive chemosensors have a long response time.³⁷ In our case, the response of **J** to Zn^{2+} was found to be very fast. After addition of the solution of Zn^{2+} , the fluorescence emission intensity of **J** in DMSO/ H_2O (pH = 7.2, v/v = 4:1) HEPES buffer solutions at 498 nm increased rapidly below 3 s. This result suggested that the recognition profiles of sensor **J** with Zn^{2+} was completed nearly instantaneously.

The pH dependence of the fluorescence intensity of **J** – Zn²⁺ system in aqueous media was examined by fluorescence emission spectroscopy. The solution of Zn²⁺ was added to a solution of sensor **J** (2×10^{-5} M) in DMSO/H₂O (pH = 7.2, v/v = 4:1) HEPES buffer solutions at pH values ranging from 1 to 13 ranges (Figure S 6) The **J** – Zn²⁺ complex showed a significant fluorescence response between pH 5 and 11, which included the physiologically relevant range of pH 7.0–8.4. In conclusion, Zn²⁺ could be clearly detected by the fluorescence spectral measurement using **J** within the physiological pH range (pH = 7.0–8.4).

In order to investigate the reversibility of the sensor **J**, the addition of Zn²⁺ (4×10^{-4} M) to the solution of sensor **J** (2×10^{-5} M) led to fluorescence increasing, that was, “on”. When adding EDTA into the solution of **J** – Zn²⁺ complex, **J** exhibited weak fluorescence, that was, “off”. Hence, this “off–on–off” switching process could be repeated several times with little fluorescent efficiency loss. The minimum decrease value of fluorescent intensity was only about 20 a. u. as shown in Figure 4

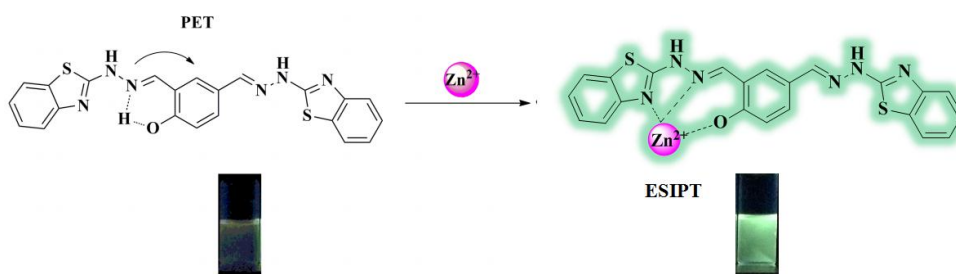
Figure 4 Reversible switching cycles of fluorescence intensity in DMSO/H₂O (pH = 7.2, v/v = 4:1) HEPES buffer solutions. ($\lambda_{\text{ex}} = 364$ nm)

The interaction mechanism between **J** (1×10^{-2} M) and Zn²⁺ (1 M) was studied by ¹H NMR titration experiments. As shown in Figure 5 the sensor **J** showed three single peaks at 12.24 ppm, 10.87 ppm and 8.48 ppm in DMSO-*d*₆, which were respectively confirmed to be the protons of –OH, –NH=N and –CH=N. Upon the addition of Zn²⁺, the signal peak of the –OH at 12.24 ppm disappeared. The job plot between **J** and Zn²⁺ was implemented. As shown in Figure S 7, the

maximum point appeared at a mole fraction of 0.5, which indicated that it was a 1:1 stoichiometry of the binding mode of **J** (2×10^{-5} M) and Zn^{2+} (1×10^{-2} M). In addition, the complex J-Zn^{2+} was subjected to mass spectral analyses. The ion peak was detected at m/z 508.54 (Figure S 8), which corresponded to $[\text{J+Zn}^{2+}]$.

Figure 5 Partial ^1H NMR spectra (400 MHz, $\text{DMSO-}d_6$) of free **J** and in the presence of varying amounts of Zn^{2+} .

In conclusion, because of the transition of the lone pair electrons ($-\text{C}=\text{N}$), free **J** only showed weak fluorescence. Upon the addition of Zn^{2+} , the deprotonation of phenolic hydroxyl group resulted in inhibiting transition of electrons and blocking the PET process. And the cooperation reaction occurred between heteroatom (N and O) of **J** and Zn^{2+} led to ESIPT process, destroyed the intramolecular hydrogen bond. As a result, **J** showed strong green fluorescence. (Scheme 2)



Scheme 2 The proposed cartoon representation of **J** for Zn^{2+} .

The selectivity and reversibility of this sensor prompted us to consider the present system as a sequence dependent molecular keypad lock using the **J**, Zn^{2+} and EDTA as three different

chemical inputs. Therefore, we made the chemical inputs designated respectively as “J”, “Z”, and “E”. In the midst of the possible six input combinations, JZE, JEZ, EJZ, EZJ, ZEJ and ZJE, the combination JZE gave minimum fluorescence output, whereas maximum output signaling was displayed by EJZ (Figure S 9). The keypad contained various keys, which the correct password order was JZE.

On the basis of the reversible fluorescent switch of **J** controlled by Zn^{2+} , and EDTA, we used it as a two-input molecular logic gate. As shown in Figure 6, when the output was zero, there were three conditions: (a) both the Zn^{2+} and EDTA were absent, (b) only EDTA was present, (c) both Zn^{2+} and EDTA were present. The output “0” corresponded to the gate being closed, which meant quenched fluorescence emission. When only Zn^{2+} alone was present, the output was one, which corresponded to the gate being open (strong fluorescence emission). Thus this repeated behavior of **J** by fluorescence change could clearly indicate the sensor was reversible and reusable for Zn^{2+} .

Figure 6 Molecular logic gate table and the respective symbolic representation of the INHIBIT logic gate function.

To investigate the practical application of chemosensor **J**, test strips were prepared by immersing filter papers into DMSO/ H_2O (pH=7.2, v/v=4:1) HEPES buffer solutions of **J** (2×10^{-4} M) and then drying in air. The test strips containing **J** were conveniently utilized to detect Zn^{2+} (2×10^{-5} M) and other metal ions. As shown in Figure 7, when Zn^{2+} were added on the test kits, the obvious color change from black to blue was observed under UV lamp (365 nm). Unsurprisingly, potentially competitive ions exerted no influence on the detection of Zn^{2+} by the

test strips. Therefore, the test strips could conveniently detect Zn^{2+} in DMSO/ H_2O (pH=7.2, v/v=4:1) HEPES buffer solutions.

Figure 7 Photographs of **J** and **J**- Zn^{2+} on test papers after immersion in DMSO/ H_2O (pH=7.2, v/v=4:1) HEPES buffer solutions. Left to right: (1) only **J**, (2) **J** with Zn^{2+} , (3) **J** with other metal ions, (2) **J**- Zn^{2+} with other metal ions under irradiation at 365 nm upon UV lamp.

Conclusions

In summary, we have developed a bi-hydrazone derivative based benzothiazole group for the selective fluorescent detection of Zn^{2+} in aqueous medium. The detection limits were 1.00×10^{-7} M and 1.64×10^{-8} M of Zn^{2+} using the visual fluorescent color changes and fluorescence spectra changes respectively, which may find potential applications for detecting micromole concentrations of Zn^{2+} in both biological systems and the environment. In addition, the fluorescence signals could be used to mimic the function of logical memory devices at the molecular level.

Experimental section

Materials and physical methods

Reagents and solvents were commercially available at analytical grade and were used without further purification. The fluorescence spectra were recorded with a Shimadzu RF-5301 spectrofluorimeter. The melting points were measured on an X-4 digital melting-point apparatus. Electrospray ionization mass spectra (ESI-MS) were measured on an Agilent 1100 LC-MSD-Trap-VL system. ^1H NMR and ^{13}C NMR spectra were recorded on a Mercury-400BB

spectrometer at 400 MHz and 100 MHz. The chemical shifts are reported in ppm down field from tetramethylsilane (TMS, δ scale with solvent resonances as internal standards).

Synthesis of sensor molecule J

The compound **J** can be readily prepared by a simple and low cost Schiff base reaction of 4-hydroxyisophthalaldehyde and 2-hydrazinylbenzothiazole (Scheme 1). 4-hydroxyisophthalaldehyde (0.7500 g, 5 mmol), 2-hydrazinylbenzothiazole (0.60 g, 5.5 mmol) and a catalytic amount of acetic acid (AcOH) were combined in hot absolute EtOH (30 mL). The solution was stirred under reflux for 4 h. After cooling to room temperature, the dark yellow precipitate was filtered, washed three times with hot absolute ethanol, then recrystallized with EtOH to obtain a yellow powdered product **J** (4.31 mmol) in 86.2% yield (m.p. >300°C). ^1H NMR (DMSO- d_6 , 400 MHz) δ : 12.24 (s, 2H), 10.87 (s, 1H), 8.48-7.01 (m, 13H,) (Figure S 1). ^{13}C NMR (DMSO- d_6 , 100 MHz) δ /ppm: 167.4, 167.1, 162.8, 158.3, 129.2, 126.7, 126.5, 126.4, 122.3, 122.1, 121.9, 120.6, 117.3. (Figure S 2) ESI-MS calcd for $[\text{C}_{18}\text{H}_{16}\text{N}_6\text{OS}_2+\text{H}^+]^+$ 445.08. Found 445.07. (Figure S 3)

Funding

This work was supported by the National Nature Science Foundation of China (No. 21467012).

References

1. Wang, M. Q.; Li, K.; Hou, J. T.; Wu, M. Y.; *J. Org. Chem.* **2012**, *77*, 8350–8354.
2. Tayade, K.; Bondhopadhyay, B.; Keshav, K.; Sahoo, S. K.; *Analyst*, **2016**, *141*, 1814–1821.

3. Leng, Y. L.; Zhang, J. H.; Li, Q.; Zhang, Y. M.; Lin, Q.; Yao, H.; Wei, T. B.; *Phosphorus Sulfur Silicon Relat. Elem.* **2016**, 191, 1318–1323.
4. Frederickson, C. J.; Bush, A. I.; *Biometals.* **2001**, 14, 353–366.
5. Liu, J. J.; Liu, H. L.; Pu, S. Z.; *J. Photoch. Photobio. A.* **2016**, 324, 14–22.
6. Berg, J. M.; Shi, Y.; *Science*, **1996**, 271, 1081–1085.
7. Gupta, V. K.; Mergu, N.; Singh, A. K.; *Sens. Actuator B Chem.* **2014**, 202, 674–682.
8. Ma, D. L.; He, H. Z.; Zhong, H. J.; Lin, S.; *Appl. Mater. Interfaces*, **2014**, 6, 14008–14015.
9. Gong, Z. L.; Zhao, B. X.; Liu, W. Y.; Lv, H. S.; *J. Photochem. Photobio. A.* **2011**, 218, 6–10.
10. Qin, J. C.; Yang, Z. Y.; *Mater. Sci. C.* **2015**, 57, 265–271.
11. Abbasi, M. A.; Ibupoto, Z. H.; Hussain, M.; Khan, Y.; *Sensor*, **2012**, 12, 15424–15437.
12. Sarkar, D.; Pramanik, A. K.; Mondal, T. K.; *J. Lumin.* **2014**, 146, 480–485.
13. Jorhem, L.; Engman, J.; *J. Aoac, Int.* **2000**, 83, 1189–1203.
14. Sreenath, K.; Clark, R. J.; Zhu, L.; *J. Org. Chem.* **2012**, 77, 8268–8279.
15. Ni, X. L.; Zeng, X.; Redshaw, C.; Yamato, T.; *J. Org. Chem.* **2011**, 76, 5696–5702.
16. Qu, W. J.; Guan, J.; Wei, T. B.; *RSC Adv.* **2016**, 6, 35804–35808.
17. Zhang, Y.; Guo, X. F.; Si, W. X.; *Org. Lett.* **2008**, 10, 473–476.
18. Xu, Z. C.; Liu, X.; Pan, J.; Spring, D. R.; *Chem Commun.* **2012**, 48, 4764–4766.
19. Wei, T. B.; Zhang, P.; Shi, B. B.; *Dyes. Pigm.* **2013**, 97, 297–302.
20. Wu, Y.; Peng, X.; Guo, B.; Fan, J.; *Org. Biomol. Chem.* **2005**, 3, 1387–1392.
21. Ma, Y. Q.; Li, G.; Su, X.; *RSC Adv.* **2015**, 5, 69251–69258.
- 22 Zhou Y.; Kim, H. N.; Yoon, J.; *Bioorg. Med. Chem. Lett.* **2010**, 20, 125–128.
- 23 Zhou, X.; Lu, Y.; Zhu, J. F.; Chan, W. H.; *Tetrahedron*, **2011**, 67, 3412–3419.

24. Dong, W. K.; Li, X. L.; Wang, L.; Zhang, Y.; Ding, Y. J.; *Sens. Actuator B Chem.* **2016**, 229, 370–378.
25. Kopchuk, D. S.; Prokhorov, A. M.; Slepukhin, P. A.; Kozhevnikov, D. N.; *Tetrahedron Lett.* **2012**, 53, 6265–6268.
26. Hu, J. H.; Li, J. B.; Qi, J., Sun, Y.; *Sens. Actuators B*, **2015**, 208, 581–587.
27. Dhaka, G., Singh, J.; Kaur, N.; *Inorg. Chim. Acta*, **2016**, 450, 380–385.
28. Gwon, S. Y.; Lee, S. Y.; Son, Y. A.; Kim, S. H.; *Fiber. Polym.* **2012**, 13 1101–1104.
29. Hu, J. H.; Li, J. B.; Qi, J.; Sun, Y.; *Phosphorus Sulfur Silicon Relat. Elem.* **2016**, 191, 984–987.
30. Hu, J. H.; Li, J. B.; Qi, J.; Sun, Y.; *New J. Chem.* **2015**, 39, 4041–4046.
31. Hu, J. H.; Wang, L. C.; Liu, H.; Wei, T. B.; *Phosphorus Sulfur Silicon Relat. Elem.* **2006**, 181, 2691–2698.
32. Sun, Y.; Hu, J. H.; Li, J. B.; Qi, J.; *Spectrochim. Act. A.* **2016**, 167,101–105.
33. Lin, Q.; Cai, Y.; Li, Q.; Chang, J.; Yao, H.; Zhang, Y. M.; Wei, T. B.; *New J. Chem.* **2015**, 39, 4162–4167.
34. Tayade, K.; Sahoo, S.; Bondehopadhyay, B.; Bhardwaj, V. K.; Singh, N.; Basu, A.; Bendre, R.; Kuwar, A.; *Biosens. Bioelectron.* **2014**, 61, 429–433.
35. Saleem, M.; Lee, K. H.; *Dyes. Pigm.* **2015**, 5, 72150–72287.
36. Y. Liu; You, C. C.; Zhang, H. Y.; *Supramol. Chem.* **2001**, 613–620.
37. Lin, Q.; Zhu, X.; Fu, Y. P.; Yang, Q. P.; Sun, B.; Wei, T. B.; Zhang, Y. M.; *Dyes. Pigm.* **2015**, 113, 748–753.

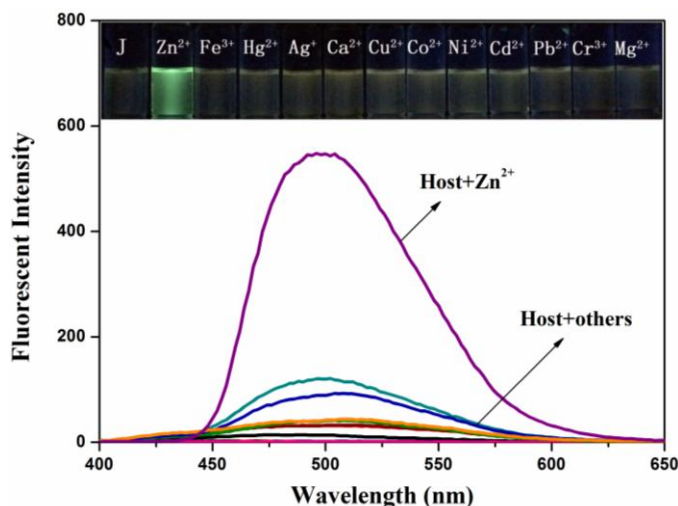


Figure 1 (a) Fluorescence emission data for **J** and in the presence of various metal ions in DMSO/H₂O (pH = 7.2, v/v = 4:1) HEPES buffer solutions. ($\lambda_{\text{ex}} = 364$ nm). (b) Color changes observed upon the addition of various cations (20 equiv.) to solutions of sensor **J** (2×10^{-5} M) in DMSO/H₂O (pH = 7.2, v/v = 4:1) HEPES buffer solutions.

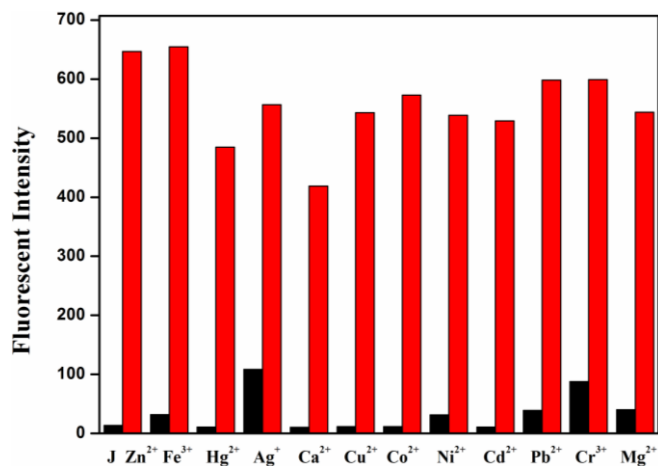


Figure 2 Fluorescence intensity changes of the **J** (20 μ M) to Zn²⁺ (20 equiv.) in the presence of various test cations (20 equiv.) in DMSO/H₂O (pH = 7.2, v/v = 4:1) HEPES buffer solutions.

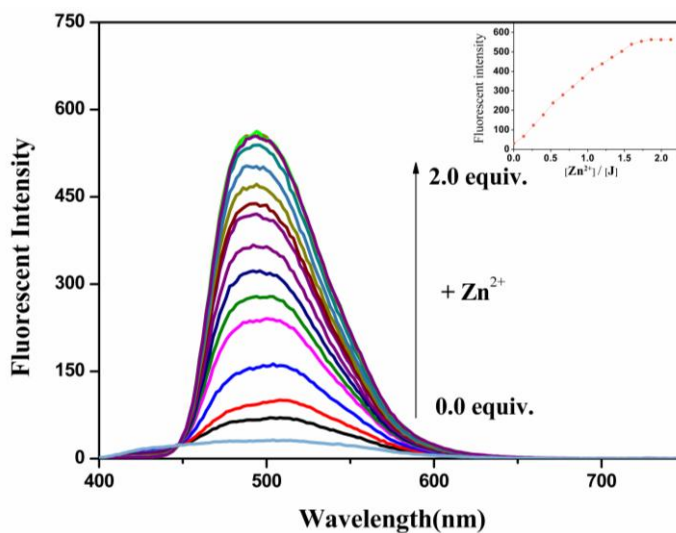


Figure 3 Fluorescence spectra of **J** (20 μ M) in the presence of different concentration of Zn^{2+} (0.0 – 2.0 equiv.) in DMSO/H₂O (pH = 7.2, v/v = 4:1) HEPES buffer solutions. Inset shows a plot of fluorescence intensity depending on the concentration of Zn^{2+} in the range from 0 to 2 equivalents.

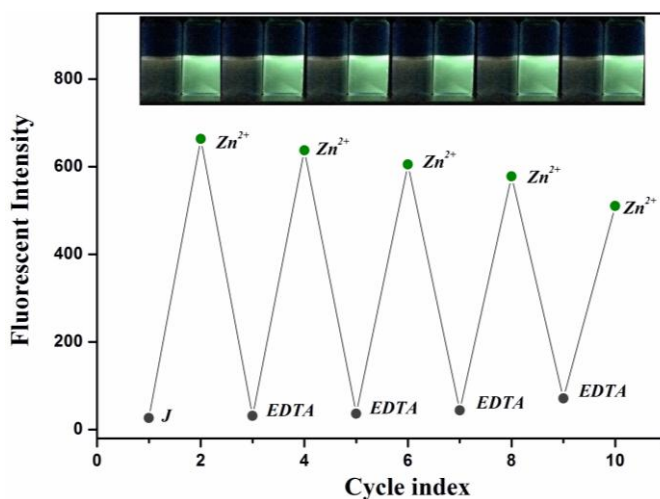


Figure 4 Reversible switching cycles of fluorescence intensity in DMSO/H₂O (pH = 7.2, v/v = 4:1) HEPES buffer solutions. ($\lambda_{\text{ex}} = 364 \text{ nm}$)

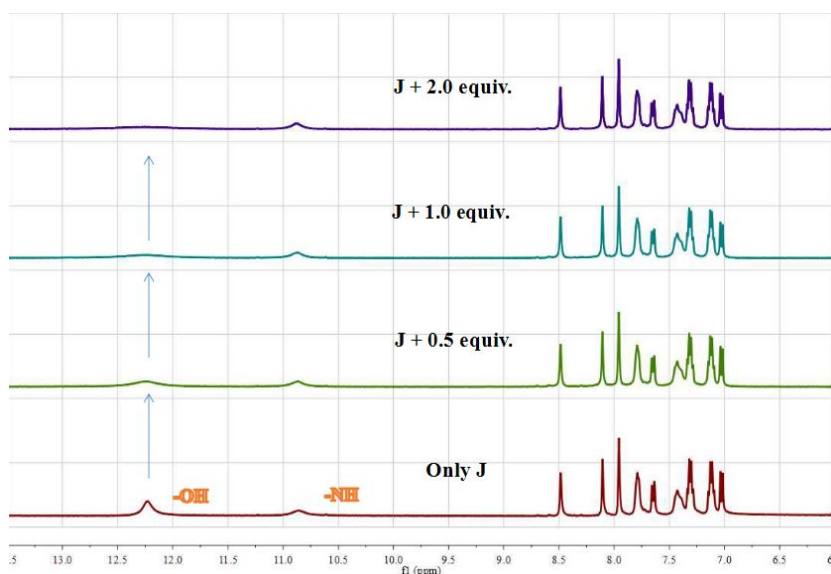
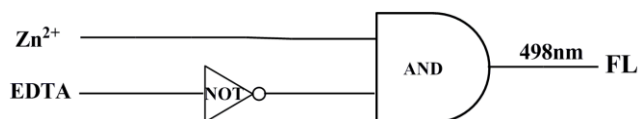


Figure 5 Partial ¹H NMR spectra (400 MHz, DMSO-*d*₆) of free **J** and in the presence of varying amounts of Zn²⁺.



Input		Output ^a
Zn ²⁺	EDTA	$\lambda_{\text{em}}=498\text{nm}$
0	0	0
1	0	1
0	1	0
1	1	0

Figure 6 Molecular logic gate table and the respective symbolic representation of the INHIBIT logic gate function.

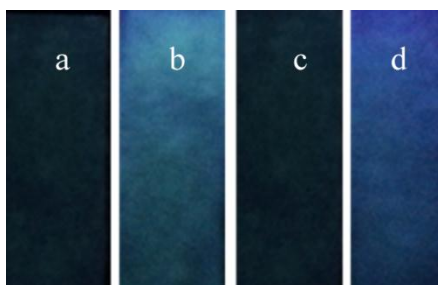


Figure 7 Photographs of **J** and **J-Zn²⁺** on test papers after immersion in DMSO/H₂O (pH = 7.2, v/v = 4:1) HEPES buffer solutions. Left to right: (1) only **J**, (2) **J** with Zn²⁺, (3) **J** with other metal ions, (2) **J-Zn²⁺** with other metal ions under irradiation at 365 nm upon UV lamp.